Research on Engineering Structures & Materials
www.jresm.org
MIM Research Group

Research Article

Experimental investigation of section bending and twisting resistance of I-Box web beams with constant steel area

Noorulhuda K.H. Al-Musawi [1,a], Najla'a Hameed Abbas [2,b], Zaidoon Saad Hameed [3,c], Zaid Mohammed Abbas [*,4,d]

[1]*College of Engineering, University of Warith Al-Anbiyaa, Karbala, Iraq*
[2]*Department of Civil Engineering University Of Babylon, Hilla, Iraq, Department of Civil Engineering University Warith Al-Anbiyaa, Karbala, Iraq*
[3]*College of Engineering, University of Warith Al-Anbiyaa, Karbala, Iraq*
[4]*Department of Civil Engineering, University of Babylon, Hilla, Iraq*

Article Info

Article History:

Received 17 Jan 2026
Accepted 14 May 2026

Keywords:

Cold-formed steel;
I-Box Web Beam;
Built-up sections;
Torsional behavior;
Concrete infill;
Width-to-depth ratio;
Composite action;
Bending–torsion interaction

Abstract

Two experimental series of short-span IBWB specimens fabricated from 3-mm-thick steel plates were tested to evaluate their behavior under combined bending and torsion. Series 1 comprised hollow IBWB sections, while Series 2 included identical specimens with box webs filled with normal-strength concrete to investigate composite action. The width-to-depth (W/D) ratio varied from 0.70 to 1.30 while maintaining a constant steel area, ensuring that geometric effects could be isolated. All specimens were subjected to identical loading conditions. For the hollow beams, increasing the W/D ratio significantly enhanced torsional performance. Specimens with W/D ratios of 1.30 and 1.15 achieved increases in torsional capacity of 76.27% and 26.32%, respectively, relative to the control beam. Conversely, specimens with lower W/D ratios (0.85 and 0.70) showed only minor strength improvements or slight reductions and consistently exhibited lower rotation capacities, indicating reduced ductility. The concrete-filled specimens demonstrated the beneficial effects of composite action. The beam with W/D = 1.30 achieved a 25.91% increase in torsional strength and a rotation angle exceedingly twice that of its hollow counterpart, indicating substantial improvements in both strength and ductility. Although some concrete-filled specimens experienced slight reductions in torsional strength, they generally displayed enhanced deformation capacity. Compared with equivalent hollow sections, all concrete-filled beams exhibited significant increases in torsional capacity, ranging from 182% to 213%. Overall, geometric configuration strongly influenced torsional behavior. Higher W/D ratios improved strength and stiffness, while lower ratios provided limited benefits. Concrete infill markedly enhanced torsional resistance, delayed local buckling, and improved overall structural performance, particularly in specimens with larger W/D ratios.

1. Introduction

The Thin-walled cold-formed steel (CFS) is increasingly adopted in structural applications because of the rising demand for members that provide high strength with low weight while effectively fulfilling their intended functions. In recent years, the use of built-up CFS sections has gained significant popularity, particularly in developing countries. CFS sheets can be manufactured into a wide range of geometric shapes and may be used either as individual sections or connected together to form built-up assemblies. Structural steel sheets are produced in various grades,

*Corresponding author: zaid.mohammed.engh331@student.uobabylon.edu.iq
[a]orcid.org/0009-0001-7862-9613; [b]orcid.org/0000-0002-1767-7291; [c]orcid.org/0009-0002-2933-9916; [d]orcid.org/0009-0004-0280-4915
DOI: http://dx.doi.org/10.17515/resm2026-1471me0117rs

ranging from low- to high-tensile strength, and are readily Hybrid girders are commercially available [1,2] and are defined as beams made from different steel grades in the flanges and the web. In this study, this concept is implemented by using higher-strength steel for the flanges relative to the web. Eurocode 3-1-3 provides guidelines for hybrid girders, stating that the ratio of the basic yield strength of the flanges to that of the web should not exceed 2. The built-up cold-formed steel (CFS) I-Box Web Beam (IBWB) section examined here consists of four individual components assembled into a single structural unit. The flanges are formed from plain channel sections with a single intermediate stiffener, while the web is constructed from a lipped channel section. These components are joined together using bolted connections fasteners. For homogeneous IBWB sections, both the webs and flanges are fabricated from low-tensile steel plates of the same grade. In contrast, the Hybrid I-Box Web Beam (IBWB) sections utilize low-tensile steel plates for the webs, whereas the flanges are fabricated from either medium- or high-tensile steel plates [3]. More broadly, the principle that optimizing material composition and component ratios yields measurable improvements in structural performance has been demonstrated across various composite civil engineering systems

This study aims to explore the behavior of an I-section double-web CFST beam under torsion and bending, focusing on the parameters addressed in this research, as detailed below.

- 1. Experimentally evaluate the torsional behavior of hollow and concrete-filled cold-formed steel box-web beams.
- 2. evaluates how variations in width-to-depth ratio, steel area, and concrete infill affect torsional stiffness and ultimate capacity.
- 3. The compressive strength and density of concrete influence its torsional response. It aims to understand these relationships to enhance the performance of steel concrete structures under torsional loads.
- 4. Investigating the structural behavior of the proposed IBWB section under torsional loading
- 5. comparing the torsional performance and stiffness characteristics with those of conventional sections.

1.1 Research Background

Existing design codes do not provide provisions for the design of built-up closed-form cold-formed steel (CFS) members, underscoring the need for further research to better understand their structural behavior. Accordingly, a brief review of previous studies relevant to the present investigation is summarized below. A numerical study on CFS built-up beams with perforated webs showed that web openings had a more pronounced effect on the strength of beams with built-up closed sections compared to those with open sections [4].

Four-point bending and torsion tests were conducted to examine the in-plane behavior of thin-walled, cold-formed built-up box beams composed of nested C- and U-shaped sections. The results indicated that, at mid-span, the components of the built-up box beams acted integrally to resist combined torsion. Additionally, it was recommended that the strong-axis bending moment capacity of built-up box beams be taken as 90% of the sum of the individual component capacities [5-7]. Experimental and numerical investigations on laterally restrained cold-formed steel rectangular hollow flange beams (RHFBs) revealed that variations in yield strength between the tubular flanges and the web significantly influenced flexural performance, promoting local buckling and plastic deformation in the web.

The inclusion of an intermediate stiffener in the external plates of the hollow flanges was found to enhance the critical local buckling capacity of the plates [8]. Finite element analysis (FEA) was employed to study the bending strength of built-up box sections commonly used in residential and commercial construction in North America [9].

The study showed that closed-form built-up sections exhibit higher torsional rigidity and that design equations based on the modified Direct Strength Method (DSM) [12] tend to be overly conservative for these sections. Additional numerical studies indicated that, under concentric loading, the flexural strength of built-up box sections can be reasonably approximated as the algebraic sum of the nominal strengths of the individual components. However, this approach was

found to be unconservative under eccentric loading, for which a reduction factor of 0.9 was recommended [10,11].

Other studies highlighted that hybrid sections outperform homogeneous sections in terms of strength. Specifically, I-sections achieve higher bending resistance with reduced cross-sectional area while effectively resisting large longitudinal shear forces [13]. Experimental and numerical investigations also revealed that built-up closed-form sections offer a higher strength-to-weight ratio than open mono-symmetric sections. Open sections typically fail by lateral–torsional buckling, whereas closed sections are more prone to distortional buckling [14,15].

Research on built-up I-beams identified steel grade, flange slenderness ratio, and the effective width-to-thickness ratio of compression flanges as key parameters controlling flexural capacity [16]. Moreover, the use of high-strength steel (HSS) was found to be advantageous in enhancing structural capacity, particularly when web depth is limited [17].

Overall, the literature shows that studies on hybrid and closed-form built-up sections remain limited. Given the widespread use of hybrid girders and built-up members in practice, further investigation is warranted, along with the development of appropriate design provisions in codes and handbooks [18,19]. The present study aims to address this gap. Based on experimental findings and parametric analyses, several conclusions were drawn. The fabricated test specimens and the cross-sectional configurations of IBWB sections with varying width-to-depth (W/D) ratios are shown in Figure 1.

2. Experimental Investigation

The experimental study on built-up cold-formed steel (CFS) IBWB sections was conducted at the Advanced Structural Engineering Laboratory, Engineering College, Babylon University, Iraq. A specialized and uniquely designed test setup was fabricated to perform combined torsional tests on short-span beam specimens.

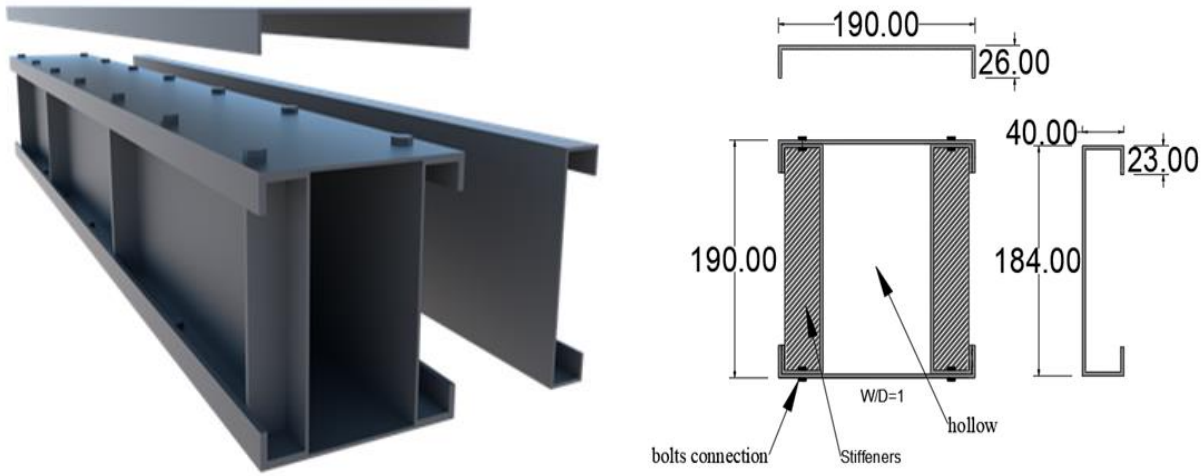

Fig. 1. I-Box Web Beam (IBWB) sections Actual cross-section and (d) Varying W/D ratios with constant steel area compared with control specimen.

2.1 Test Specimens

Two series of tests were conducted using box sections with different strength levels. Each series comprised five specimens with varying width-to-depth (W/D) ratios, while maintaining a constant steel area relative to the control specimens.

Series 1 consists of thin-walled homogeneous IBWB sections, in which both the flanges and webs were made from low-tensile-strength steel sheets of the same grade. Series 2 comprises sections identical to those in Series 1, except that the box web was infilled with normal concrete. For all specimens, the web thickness (tw) was 3.0 mm, and the flange thickness was also 3.0 mm.

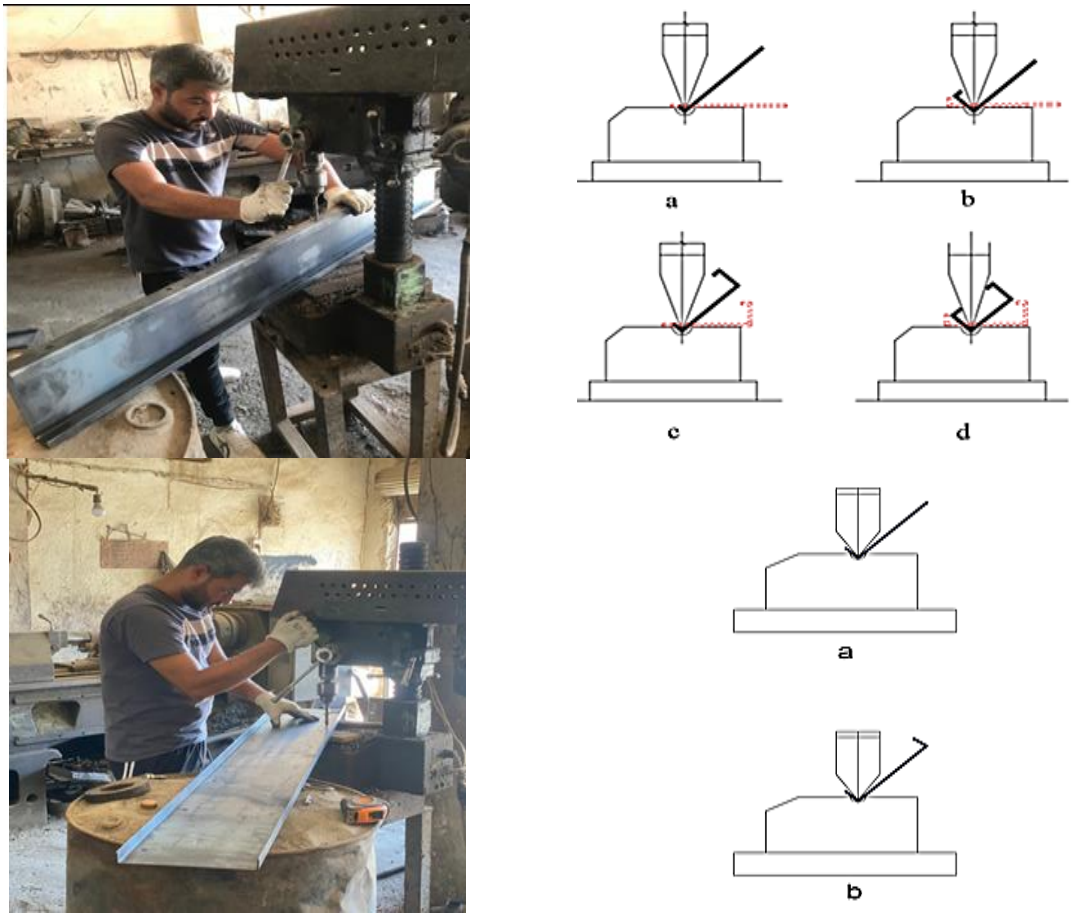

Fig. 2. Connecting parts of sections

Table 1. Identification for specimen dimensions

Specimen identification	Description
BH 1	CFS I-beam with rectangular hollow Web (W=190mm, D=190mm)
BC 1	CFS I-beam with rectangular hollow Web filled with concrete (W=190mm, D=190mm)

Table 2. Details for cross-section of specimens of control specimen

Specimen identification	D mm	W mm	W/D	t_w mm	t_f mm	Location of connection	A_s mm^2	A_c mm^2
Control Specimen	190	190	1	3	3	L/6	4860	19136

Table 3. Identification for flange depth of Series 1

Specimen identification	Description
BH1.3	CFS I-beam with constant area of steel compared with control specimen and hollow box Web (W=202mm, D=175mm)
BH 1.15	CFS I-beam with constant area of steel compared with control specimen and hollow box Web (W=202mm, D=175mm)
BH 0.85	CFS I-beam with constant area of steel compared with control specimen and hollow box hollow Web (W=175mm, D=204mm)
BH 0.7	CFS I-beam with constant area of steel compared with control specimen and hollow box hollow Web (W=155mm, D=221mm)

Table 4. Details for cross-section of specimens of Series 1

Specimen identification	D mm	W mm	W/D	t_w mm	t_f mm	Location of connection	A_s mm²
BH1.3	163	211	1.3	3	3	L/6	4860
BH 1.15	175	202	1.15	3	3	L/6	4860
BH 0.85	204	175	0.85	3	3	L/6	4860
BH 0.7	221	155	0.7	3	3	L/6	4860

Table 5. Identification for flange depth of Series 2

Specimen identification	Description
BC1.3	CFS I-beam with constant area of steel compared with control specimen and concrete in side of box Web (W=202mm, D=175mm)
BC 1.15	CFS I-beam with constant area of steel compared with control specimen and concrete in side of box Web (W=202mm, D=175mm)
BC 0.85	CFS I-beam with constant area of steel compared with control specimen and concrete in side of box hollow Web (W=175mm, D=204mm)
BC 0.7	CFS I-beam with constant area of steel compared with control specimen and concrete in side of box hollow Web (W=155mm, D=221mm)

Table 6. Details for cross-section of specimens of Series 2

Specimen identification	D mm	mm	W/D	t_w mm	t_f mm	Location of connection	A_s mm²	A_c mm²
BC1.3	163	211	1.3	3	3	L/6	4860	20618
BC 1.15	175	202	1.15	3	3	L/6	4860	19604
BC 0.85	204	175	0.85	3	3	L/6	4860	17622
BC 0.7	221	155	0.7	3	3	L/6	4860	14835

The width-to-depth (W/D) ratios of the beams—0.70, 0.85, 1.00, 1.15, and 1.30—are indicated at the end of the specimen nomenclature. Table 1 presents Identification for Specimen dimensions. Series 1 has a constant steel area equal to that of the control specimen, and all details regarding the identification and dimensions of these specimens are presented in Tables (3 and 4). Series 2 has the same cross-sectional details and dimensions as Series 1, with the only difference being the area of the web filled with normal concrete.

2.2 Mechanical Properties

Since built-up hybrid beams are fabricated using steels of different grades, accurate determination of their mechanical properties and corresponding stress–strain relationships are essential. The compressive strength of the concrete infill used in Series 2 (f'c ≈ 36 MPa) was verified through standard testing; non-destructive methods such as ultrasonic pulse velocity has also been widely employed for in-situ concrete strength assessment [20]. Accordingly, a series of coupon tests was conducted to evaluate the mechanical characteristics of the various steel grades employed in fabricating These sections were tested, and the resulting stress–strain curves and material properties were then used to estimate the moment capacities of the built-up members, and the young's modulus for concrete for normal concrete is E=4700$\sqrt{f'c}$.

The tensile test specimens were prepared in accordance with the dimensions shown in Figure 3, with all coupons having a thickness of 3 mm. Coupon testing represents a standard approach for evaluating the mechanical behavior of metallic materials under tensile loading, with results directly informing structural capacity predictions [21]. The tests were carried out in the Mechanical Engineering Laboratory at the University of Babylon. The test setup, including the gripping arrangement and the tested specimens, is illustrated in Figure 4. The outcomes of the tensile tests—namely the yield strength and ultimate tensile strength of the flange and web materials—are summarized in Table 7.

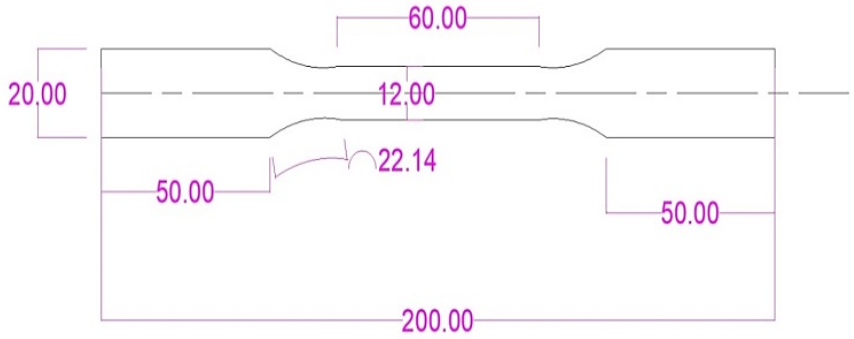

Fig. 3. Dimensions of the tensile test specimen (thickness = 3 mm). According to ASTM.

Fig. 4.Tensile testing machine with mounted specimen and tested coupons.

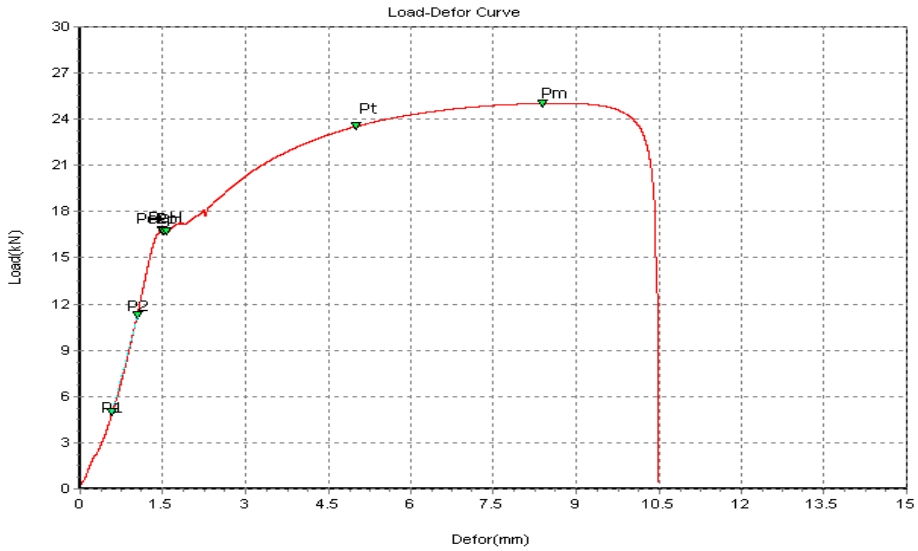

Fig 5. Load–deformation curve of steel coupons obtained from tensile testing

Table 7. Yield and ultimate tensile stress values of steel plate coupons (flanges and webs).

Specimen NO	Yield stress (MPa)	Ultimate strength (Mpa)	Young's modulus (GPa)
1	225	295	
2	230	305	200
Average value	227.5	300	

2.3 Test Set-Up and Procedure

During testing, the overall structural response of each beam specimen was carefully The specimens were monitored at every stage of loading. Testing was performed using a universal testing machine

with a maximum capacity of 30 tons. A two-point loading configuration was employed to induce combined torsion, with a torsional moment arm of 450 mm corresponding to the applied torque. Two linear variable differential transformers (LVDTs) were installed on the torque arms to measure the angle of twist, while an additional LVDT was positioned at midspan to record vertical deflection. The beams were subjected to combined bending and torsion under a constant loading rate. The load at the onset of the first crack was recorded, and the development of cracks and the failure mode were continuously observed [22-24]

It should be noted that the loading procedure and the positioning of the specially fabricated specimens required significant care. Since the supports allowed free rotation, achieving proper balance of the specimens was challenging and necessitated careful handling. All specimens were tested under progressively increasing torque until failure. The load was applied incrementally, with instrument readings recorded manually throughout the test. At each load increment, strains in both the tension and compression zones were measured using strain gauges connected to a data acquisition system and a computer was gradually increased until ultimate failure occurred. The experimental setup and instrumentation employed in the tests are shown in Figure 6.

Fig. 6. Member under Torsional load

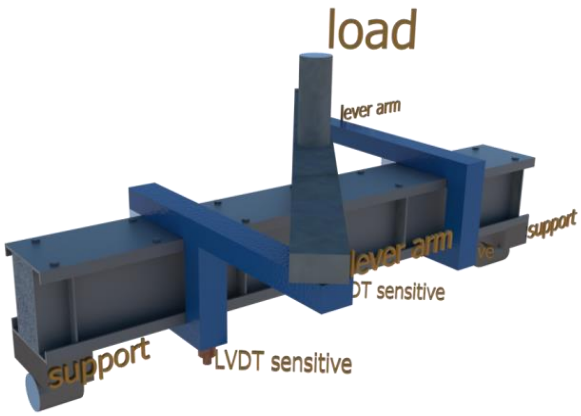

Fig. 7. Location of LVDT sensors

3. Results and Discussion

The applied bending moment was determined by multiplying the measured load by the distance between the support and the point of load application. In the built-up sections, the web elements were consistently classified as non-compact (NC), whereas the flanges were either slender (S) or non-compact. Consequently, the assembled IBWB sections were categorized as either non-compact or slender based on their controlling slenderness criteria of the flanges. Table (8) summarizes the overall behavior of the tested cold-formed steel box-web specimens, presenting critical parameters such as the maximum torque capacity, ultimate rotation, and mid-span deflection for each beam. These results form the basis for comparative analysis across different Series, which were designed to investigate the influence of geometric and material variations on structural response.

Table 8. Experimental Results of specimens in Series 1 and Series 2

Group name	Symbol number	Ultimate Load (kN)	Ultimate torque applied (kN.m)	Ultimate rotation (rad)	Increasing the load carrying capacity %	Mid-span deflection (mm)
Series 1	BH1.3	130.064	29.2644	0.0357755	76.27	13.107692
	BH 1.15	93.208	20.972	0.025435	26.32	13.530939
	BH 1	73.7831	16.6012	0.0360654	-----	16.41514
	BH 0.85	72.259	16.2583	0.0247104	-2.06	16.64468
	BH 0.7	81.214	18.2732	0.0356199	9.98	17.32698

Group name	Symbol number	Ultimate Load (kN)	Ultimate torque applied (kN.m)	Ultimate rotation (rad)	Increasing the load carrying capacity %	Mid-span deflection (mm)
Series 2	BC1.3	259.542	58.397	0.07636	25.91	12.711599
	BC 1.15	185.016	41.6286	0.0550257	-10.24	14.954822
	BC 1	206.131	46.3796	0.0376851	-----	17.526251
	BC 0.85	132.113	29.7256	0.0317171	-35.9	15.535042
	BC 0.7	173.120	38.9526	0.0356381	-16.01	15.824175

3.1 Series 1

Figure 8 presents the torque–rotation curves obtained for all specimens within this Series 1 together with an integrated comparative analysis. The key findings are as follows:

- Beams with W/D > 1 (BH1.3, BH1.15): These specimens exhibited a significant increase in torsional strength compared with the control. BH1.3 showed a 76.3% increase in Tu, while BH1.15 achieved a 26.3% increase. However, their ultimate rotation was slightly reduced, indicating higher stiffness but reduced ductility.
- Beams with W/D < 1 (BH0.85, BH0.7): The response was less favorable. BH0.85 recorded a slight reduction in Tu (−2.1%) relative to the control, whereas BH0.7 achieved a modest increase of +9.98%. In both cases, the ultimate rotation was lower than that of the control, suggesting limited ductility.

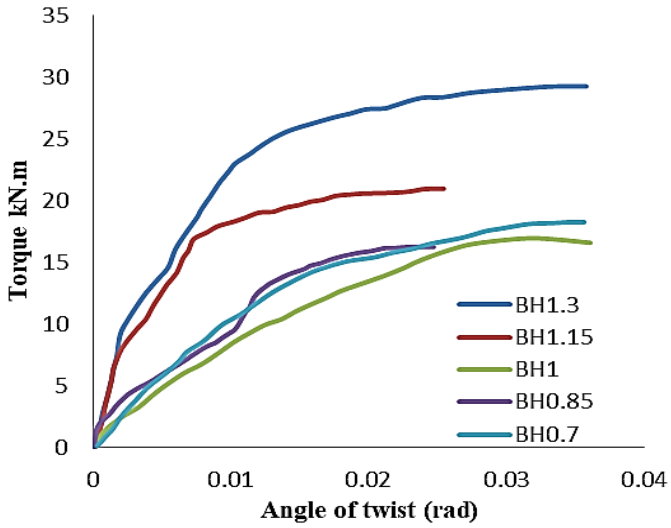

Fig. 8. Torque -Rotation curves for Series 1

- Failure modes: Consistent with the earlier groups, torsional buckling was the dominant mechanism of failure Figure (9 to 13). Figure 8 compares the torque–rotation curves of all specimens in Group 3: Steeper initial slopes for BH1.3 and BH1.15 reflect higher torsional stiffness (K ∝ GJ), as the increase in W/D improved the torsional constant (J) without increasing the overall steel area. Higher torque capacity but reduced twist capacity: The larger W/D ratios effectively delayed buckling and increased strength, but this enhancement was accompanied by reduced ultimate rotation, consistent with the trade-off between stiffness and ductility. Specimens with W/D < 1 (BH0.85 and BH0.7) failed to develop both strength and ductility compared to the control. The lower J associated with smaller widths limited torsional resistance, while constant steel area did not provide additional confinement or stiffness to compensate for this deficiency.

Fig. 9. Failure Mode of Beam BH1.3

Fig. 10. Failure Mode of Beam BH1.15

Fig. 11. Failure Mode of Beam BH1

Fig 12. Failure Mode of Beam BH0.85

Fig 13. Failure Mode of Beam BH0.7

The findings of Series 1 carry several implications for real-world design: Design balance between strength and ductility: Beams with W/D ≥ 1.15 demonstrated improved torsional strength but reduced rotational capacity. This highlights the importance of balancing geometry to ensure that enhanced strength does not come at the expense of brittle behavior. Limitations of low W/D designs: Beams with W/D < 1 are not suitable for torsion-dominated applications, as they provide neither adequate strength nor sufficient ductility. Constant steel area sections reflect cost-efficiency trade-offs: By maintaining the same steel area, Series 1 illustrates that geometric optimization (via W/D) can modestly improve performance without increasing material cost.

3.2 Series 2

This Series examined the behavior of cold-formed steel box-web beams with constant steel area but filled with nonstructural concrete (f'c ≈ 36 MPa). Five specimens were tested: BC1.3, BC1.15, BC0.85, BC0.7, and the control beam BC1 (W/D = 1). The geometry was identical to Group 3, but with the addition of concrete infill to assess the impact of composite action under torsional loading. Experimental Observations The torque–rotation relationships are shown individually in Figures 14 to 18, with a comparative overview in Figure 14. Key findings include: Enhanced torsional strength: Beams with higher W/D ratios demonstrated superior torsional strength compared to the control. BC1.3 exceeded BC1 by +25.9%, while BC1.15 recorded a slight reduction (−10.2%) in Tu. The control beam BC1 itself exhibited a very high torsional strength relative to hollow sections (279% higher than BH1). Reduced or variable rotation capacity: BC1.3 showed a significant increase in ultimate rotation (+105%), while BC1.15 exhibited improved ductility (+48.6%). Conversely, beams with smaller W/D ratios (BC0.85, BC0.7) recorded both lower Tu and reduced rotation compared to the control. Failure modes: Figure (20 to 24) confirm that torsional buckling governed the response, but concrete infill enhanced resistance to local buckling and provided additional confinement. Figure 14 highlights the combined performance of Series 2 beams. Concrete infill as a strength enhancer: Compared to their hollow counterparts in Series 1, the concrete-filled beams achieved substantially higher torsional resistance. For example, BC1.3 achieved +197% higher Tu than BH1.3. This enhancement is explained by the composite action: the steel box resists and confines the concrete, while the concrete delays local buckling of the thin steel walls and increases energy absorption.

Strength–ductility trade-off: While torsional strength increased with concrete infill, ductility did not always follow the same trend. For instance, BC1.3 combined high strength and exceptional ductility (θu = 0.076 rad), whereas BC0.85 suffered reductions in both Tu and θu. This indicates that geometry (W/D) still plays a critical role even in composite sections. Low W/D performance: Beams with W/D < 1 (BC0.85, BC0.7) could not achieve the same improvements. Despite the presence of concrete, the reduction in torsional stiffness due to geometry (low J) limited their effectiveness. Explanation of Behavior Composite effect: The confinement of concrete by the steel box improved torsional resistance, stiffness, and energy absorption capacity. Geometric influence: Larger W/D ratios increased the torsional constant J, amplifying the benefits of concrete infill. In contrast, small W/D ratios limited J and undermined the potential gains from concrete. Failure

mechanism: Torsional buckling was still the governing mode, but it occurred at higher torque levels due to the stabilizing effect of the concrete.

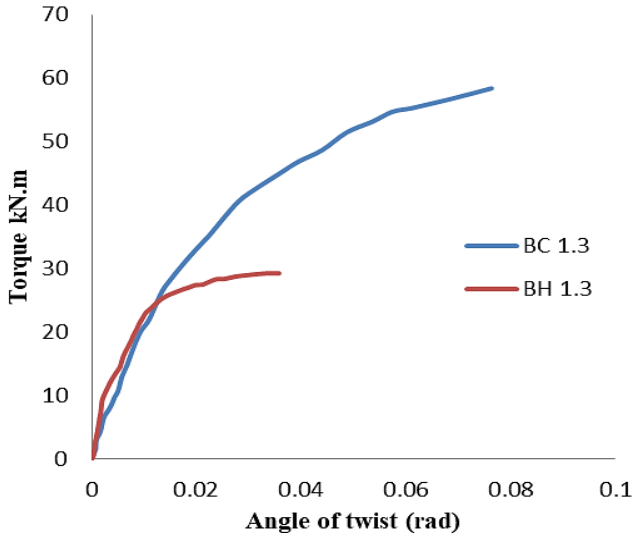

Fig 14. Torque rotation curve for beam (BC1.3)

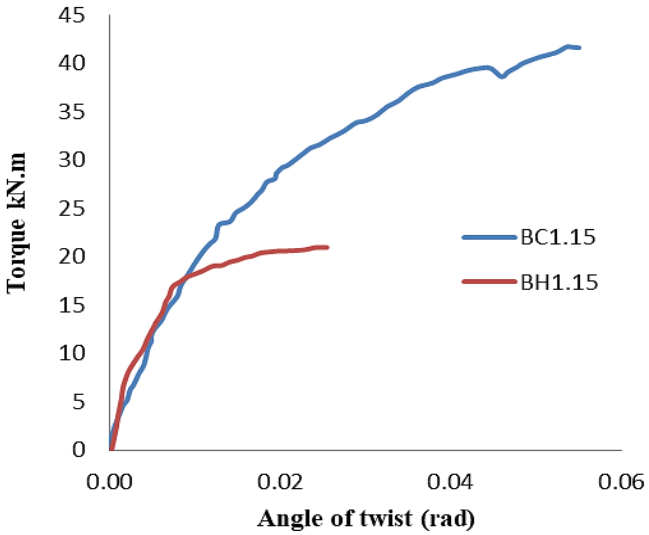

Fig 15. Torque rotation curve for beam (BC1.15)

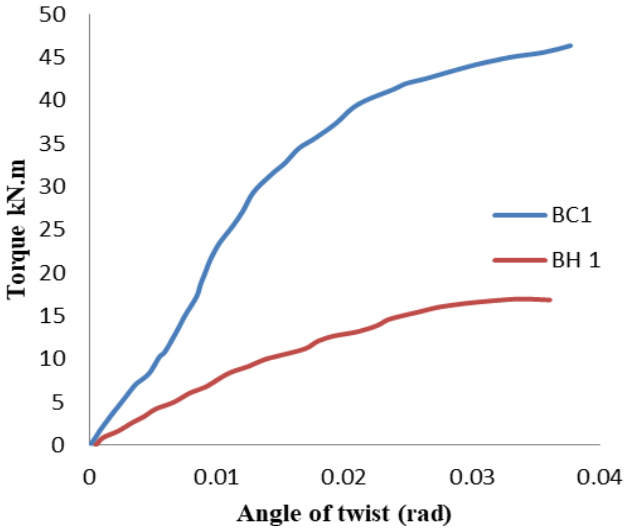

Fig 16. Torque rotation curve for beam (BC1) control beam

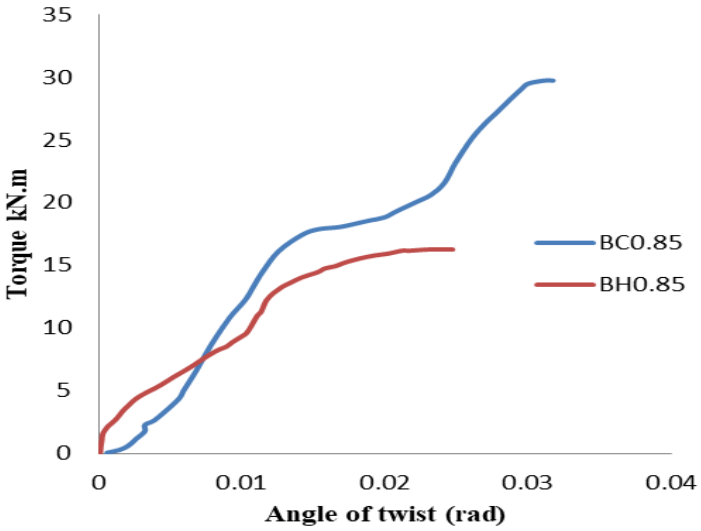

Fig 17. Torque rotation curve for beam (BC0.85)

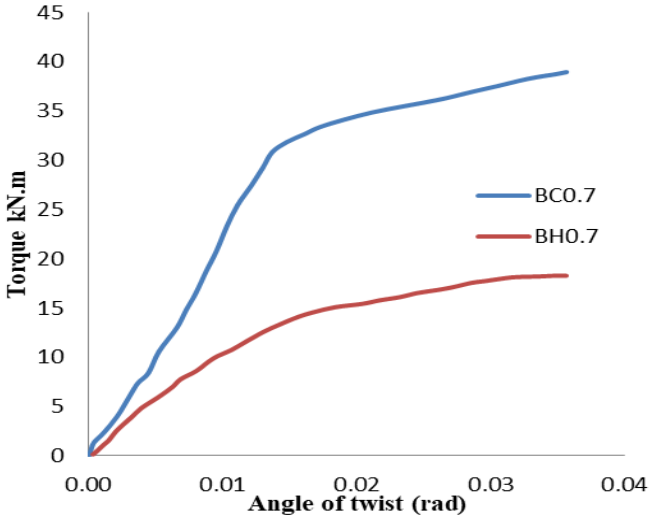

Fig 18. Torque rotation curve for beam (BC0.7)

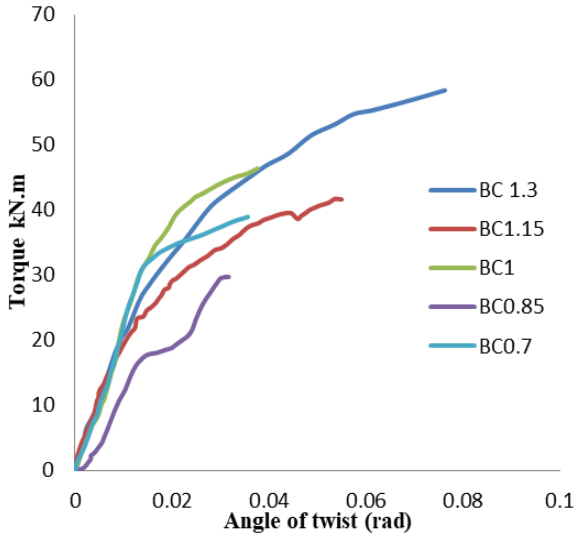

Fig 19.Torque -rotation curves for series 2

Interpretation of Figure 17 (Specimen BC0.85) Observed behavior: BC0.85 reached lower torsional strength (−35.9% vs. BC1) and smaller ultimate rotation (−16.2% vs. BC1). The curve shows a stiff

initial slope but fails early with limited ductility. Reason: The low W/D ratio (0.85) reduces the torsional constant J, limiting torque resistance. Concrete infill improved initial stiffness and delayed buckling but could not overcome the geometric disadvantage. Failure was dominated by torsional buckling at lower twist, explaining the reduced ductility. Practical Significance: The outcomes of Series 2 provide several design insights: Concrete-filled box sections are highly efficient under torsion, especially when designed with W/D ≥ 1.15. They provide superior torsional strength and, in some cases (e.g., BC1.3), exceptional ductility. Geometry remains critical: Concrete infill cannot fully compensate for the disadvantages of low W/D ratios. Designers should avoid W/D < 1 for torsion-critical applications, even when concrete is used.

Table 9. Stiffness Parameter of all specimens

Group three constant area with control hollow box	BH1.3	29.2644	0.0357755	819.71
	BH 1.15	20.972	0.025435	825.669
	BH 1	16.6012	0.0360654	461.11
	BH 0.85	16.2583	0.0247104	658.218
	BH 0.7	18.2732	0.0356199	513.286
Group four constant area with control concrete box	BC1.3	58.397	0.07636	765.36
	BC 1.15	41.6286	0.0550257	756.87
	BC 1	46.3796	0.0376851	1233.244
	BC 0.85	29.7256	0.0317171	937.53
	BC 0.7	38.9526	0.0356381	1094.15

Balanced performance: BC1.3 illustrates the ideal balance, achieving both high torsional strength and large twist capacity. Such behavior is desirable in seismic or fatigue-prone structures where both resistance and energy dissipation are required. Practical applications: These findings are directly relevant to the design of bridge girders, offshore platforms, transmission towers, and tall buildings, where torsional effects are significant. Incorporating concrete infill with optimized W/D ratios can lead to safer, stiffer, and more ductile structural systems. Torsional stiffness (K) is a fundamental parameter describing the ability of a structural element to resist angular deformation under applied torque. It is defined as the ratio of ultimate torsional moment to the corresponding ultimate angle of twist:

$$Stiffness\ (K) = Tu/\theta u \quad (1)$$

Where; Tu= ultimate torsional moment (kN·m), θu= ultimate rotation (rad).

Fig. 20. Failure mode of beam BC1.3

Fig. 21. Failure mode of beam BC1.15

Fig. 22. Failure mode of beam BC1

Fig. 23. Failure mode of beam BC0.85

Fig. 24. Failure mode of beam BC0.7

4. Conclusion

4.1 Series 1

- Effect of W/D Ratio: Increasing the W/D ratio enhances torsional capacity, with BH1.3 and BH1.15 exceeding the control by 76.27% and 26.32%, respectively.
- Effect on Rotation: Larger W/D ratios resulted in reduced rotation capacity, while smaller ratios demonstrated slight increases in twist before failure, indicating improved flexibility.
- Overall Torsion–Rotation Interaction: Variation in steel area significantly affects torsional response more than the W/D ratio when steel area remains constant.
- Best Performance: BH1.3 demonstrated the optimal balance of strength and ductility.
- Effect of Constant Steel Area: Maintaining a constant steel area improved torsional resistance responses, aligning more closely with the control specimen, thus highlighting material quantity's key role.

4.2 Series 2

- Effect of Concrete Filling: Concrete infill significantly enhanced the torsional capacity, with the control beam (BC1) demonstrating a 279.33% improvement compared to its hollow counterpart.
- Influence of W/D Ratio: BC1.3 demonstrated the highest torsional strength with a 25.9% increase and a 105.4% rise in rotation angle. BC1.15, while showing a 10.24% strength decrease, achieved a rotation improvement of 48.64%. Lower W/D ratios (BC0.85, BC0.7) led to diminished strength and twist capacity.
- Composite Behavior: The combined action of steel and concrete effectively restrained inward/outward buckling and crack propagation, improving both strength and durability.
- Constant Steel Area Effect: Fixing the steel area reduced the influence of geometry on torsional strength, highlighting differences in deformation behavior.
- Optimal Specimen: BC1.3 exhibited the best overall balance of strength and rotational capacity, confirming the advantage of larger W/D ratios combined with concrete infill.

The mechanical contribution of mineral additives to composite material matrices has been similarly reported in related civil engineering contexts [24].

References

[1] Acharya SR, Sivakumaran KS, Young B. Reinforcement schemes for cold-formed steel joists with a large web opening in shear zone-An experimental investigation. Thin-Walled Structures. 2013;72:28-36. https://doi.org/10.1016/j.tws.2013.06.011

[2] Anapayan T, Mahendran M, Mahaarachchi D. Section moment capacity tests of LiteSteel beams. Thin-Walled Structures. 2011;49:502-512. https://doi.org/10.1016/j.tws.2010.12.004

[3] European Committee for Standardization. Eurocode 3: Design of Steel Structures - Part 1-1: General Rules and Rules for Buildings (EN 1993-1-1:2005). Brussels, Belgium: European Committee for Standardization; 2005.

[4] European Committee for Standardization. Eurocode 3: Design of Steel Structures - Part 1-3: General Rules - Supplementary Rules for Cold-Formed Members and Sheeting (EN 1993-1-3:2006). Brussels, Belgium: European Committee for Standardization; 2006.

[5] European Committee for Standardization. Eurocode 3: Design of Steel Structures - Part 1-5: General Rules - Plated Structural Elements (EN 1993-1-5:2006). Brussels, Belgium: European Committee for Standardization; 2006.

[6] European Committee for Standardization. Metallic Materials - Tensile Testing - Part 1: Method of Test at Room Temperature (EN ISO 6892-1:2009). Brussels, Belgium: European Committee for Standardization; 2009.

[7] Kwon YB, Seo GH. Prediction of the flexural strengths of welded H-sections with local buckling. Thin-Walled Structures. 2012;54:126-139. https://doi.org/10.1016/j.tws.2012.02.005

[8] Abbas Z M, Abbas N H. Torsional behavior of concrete-filled cold-formed steel beams with box-shaped webs. Res. Eng. Struct. Mater., 2026; 12(1): 81-93. http://dx.doi.org/10.17515/resm2025-945me0603rs

[9] Hamza BA, Hussein WN, Al Shuraifi M. Nonlinear structural response of different web openings in composite beams reinforced with BFRB wrapping. Mathematical Modelling of Engineering Problems. 2025;12(10):3435-3446. https://doi.org/10.18280/mmep.121010

[10] Niu S, Rasmussen KJR, Fan F. Distortional global interaction buckling of stainless steel C beams: Part II - Numerical study and design. Journal of Constructional Steel Research. 2014;96:40-53. https://doi.org/10.1016/j.jcsr.2014.01.008

[11] Ali MA, Azar BF, Hadidi A, Farzam M. Numerical and experimental study of coupling beams in reinforced concrete shear walls with diagonal steel members. Reinforced Concrete Materials and Applications. 2025;35(3). https://doi.org/10.18280/rcma.350303

[12] Shokouhian M, Shi Y. Flexural strength of hybrid steel I beams based on slenderness. Engineering Structures. 2015;93:114-128. https://doi.org/10.1016/j.engstruct.2015.03.029

[13] Tondini N, Morbioli A. Cross sectional flexural capacity of cold formed laterally restrained steel rectangular hollow flange beams. Thin-Walled Structures. 2015;95:196-207. https://doi.org/10.1016/j.tws.2015.06.018

[14] Kareem YS. Improving formability of low-carbon steel shells through deep drawing: Experimental analysis using SPSS. Warith Scientific Journal of Engineering and Technology. 2025;1(1):Art. 2. https://doi.org/10.57026/wsjet.v1i1.21

[15] Wang L, Young B. Behaviour of cold-formed steel built-up sections with intermediate stiffeners under bending. I: Tests and numerical validation. Journal of Structural Engineering. 2015. [Baskıda / Erken Görünüm]. https://doi.org/10.1061/(ASCE)ST.1943-541X.0001428
[16] Wang L, Young B. Design of cold formed steel built up sections with web perforations subjected to bending. Thin-Walled Structures. 2017;120:458-469. https://doi.org/10.1016/j.tws.2017.06.016
[17] Wanniarachchi KS. Flexural behaviour and design of cold-formed beams with rectangular hollow flanges [Ph.D. dissertation]. Brisbane, QLD, Australia: Queensland University of Technology; 2005.
[18] Alsultani AS, Al Shareef NH. Flexural behavior of rectangular double hollow flange cold formed steel I beam. Tikrit Journal of Engineering Sciences. 2023;30(4):28-35. https://doi.org/10.25130/tjes.30.4.4
[19] Hashim AM, Ali AY. Restoring strength of reinforced concrete horizontally curved box beam with opening using reactive powder concrete (RPC) and FRP techniques. Mechanics, Materials Science & Engineering. 2022;9(2):359-370. https://doi.org/10.18280/mmep.090209
[20] Mahmmod LMR, Alameer SAA, Abdulrasool AT. Development of a model to estimate concrete compressive strength using ultrasonic testing based on previous models. IOP Conference Series: Materials Science and Engineering. 2021;1067:012018. https://doi.org/10.1088/1757-899X/1067/1/012018
[21] Mahmood AA, Kokz SA, Mohsen AM. The influence of ultrasonic impact peening (UIP) on the mechanical properties and fatigue life of the AA1100 alloy. Journal of Applied Engineering Science. 2023;21(2):384-391. https://doi.org/10.5937/jaes0-38125
[22] Kadhim YN, Abdulrasool AT, Dulaimi A, Pinto HAS, Bernardo LFA. Influence of walnut shell ash and limestone filler in hot mix asphalt. Journal of Composites Science. 2025;9:22. https://doi.org/10.3390/jcs9010022
[23] Dulaimi A, Kadhim YN, Al Quraishy QAA, Al Hawesah HA, Ribeiro TP, Bernardo LFA. Mechanical properties and microstructure of high-performance cold mix asphalt modified with Portland cement. CivilEng. 2025;6:46. https://doi.org/10.3390/civileng6030046
[24] Al-Araji NMH, Kashesh GJ, Dulaimi A. Effect of adding metakaolin and dolomite powder on the properties of hot mix asphalt. IOP Conference Series: Earth and Environmental Science. 2025;1507:012048. https://doi.org/10.1088/1755-1315/1507/1/012048